Accepted for publication in the Astrophysical Journal
Preprint typeset using LaTeX style emulateapj v. 08/13/06

SPECTROPOLARIMETRY OF THE UNIQUE TYPE Ib SUPERNOVA 2005bf: LARGER ASYMMETRY REVEALED BY LATER-PHASE DATA [1]

Masaomi Tanaka[2,3], Koji S. Kawabata[4], Keiichi Maeda[3], Masanori Iye[5], Takashi Hattori[6], Elena Pian[7], Ken'ichi Nomoto[3,2], Paolo A. Mazzali[8,9], and Nozomu Tominaga[10,5]

ABSTRACT

We present an optical spectropolarimetric observation of the unique Type Ib supernova (SN) 2005bf at 8 days after the second maximum. The data, combined with the polarization spectrum taken at 6 days before the second maximum (Maund et al. 2007a), enable us to closely examine the intrinsic properties of the SN. The polarization percentage is smaller at the later epoch over a wide wavelength range, while the position angle is similar at the two epochs. We find that an assumption of complete depolarization of strong lines at the emission peak is not necessarily correct. The intrinsic polarization of the SN is larger, and thus, the ejecta of SN 2005bf would be more asymmetric than previously expected. The axis ratio of the photosphere projected on the sky deviates from unity by at least 20 %. If the position angle of interstellar polarization is aligned with the spiral arm of the host galaxy, the deviation is larger than 25 %. The line polarization at the He I, Ca II and Fe II lines is also smaller at the later epoch. The changes in the position angle across these lines, which were observed at the earlier epoch, are still marginally present at the later epoch. The similar polarimetric behavior suggests that the distributions of these ions are correlated. Properties of polarization, as well as the light curve and the spectra both at photospheric and nebular phases, can be explained by an aspherical, possibly unipolar explosion of a WN star in which the blob of ^{56}Ni penetrates C+O core and stops within the He layer.

Subject headings: polarization — supernovae: individual (SN 2005bf)

1. INTRODUCTION

Asymmetry is one of the keys to understand the explosion mechanism of core-collapse supernovae (SNe). Various mechanisms that could lead to aspherical explosions have been studied, including e.g., rotation and magnetic field (e.g., Müller & Hillebrandt 1981; Yamada & Sato 1994; Takiwaki et al. 2004), convection (e.g., Burrows et al. 1995; Janka & Müller 1996) or standing accretion shock instability (e.g., Blondin et al. 2003; Iwakami et al. 2008).

Observational constraints on SN asymmetry can be obtained via direct imaging (e.g., Wang et al. 2002; Hwang et al. 2004) only for a few, very nearby SNe or supernova remnants. For extragalactic SNe, polarimetry is one of the most direct methods to study asymmetry of the explosion. Polarization is produced by electron scattering within the SN ejecta. Since the polarization vectors are canceled out in spherically symmetric ejecta, no polarization would be detected from a spherical explosion. In other words, the detection of polarization undoubtedly indicates asymmetry of the explosion (Shapiro & Sutherland 1982; McCall 1984; Höflich 1991).

Spectropolarimetry is a more powerful tool than imaging polarimetry because polarization across lines possesses information on the element distribution (see Wang & Wheeler 2008, for a recent review). Since the scattering by the line depolarizes the light, line polarization is detected when the distributions of elements or ions are not uniform (even when the underlying photosphere is spherically symmetric). The asymmetric nature of core-collapse SNe has been studied in detail by spectropolarimetry (e.g., Cropper et al. 1988; Trammell et al. 1993; Wang et al. 2001, 2003a; Leonard et al. 2001, 2002, 2006; Kawabata et al. 2002, 2003; Maund et al. 2007a,b,c; Hoffman et al. 2008; Tanaka et al. 2008a).

In this paper, we present a spectropolarimetric observation of the Type Ib SN2005bf, which appears to be a unique supernova because of the following aspects: (1) The light curves showed double peaks (Anupama et al. 2005; Tominaga et al. 2005; Folatelli et al. 2006). (2) The SN was at first classified as Type Ic (SNe without H or He lines) but then re-classified as Type Ib (SNe with He lines) because of the emergence of strong He lines (Wang & Baade 2005; Modjaz et al. 2005). (3) The decline of the luminosity after the second maximum was very rapid (Tominaga et al. 2005; Folatelli et al. 2006). In addition, the luminosity around 300 days after the explosion was much fainter than expected from $0.3M_{\odot}$ of ^{56}Ni necessary to account for the second SN luminosity

[1] Based on data collected at Subaru Telescope, which is operated by the National Astronomical Observatory of Japan.

[2] Department of Astronomy, Graduate School of Science, University of Tokyo, Bunkyo-ku, Tokyo, Japan; mtanaka@astron.s.u-tokyo.ac.jp
[3] Institute for the Physics and Mathematics of the Universe, University of Tokyo, Kashiwa, Japan
[4] Hiroshima Astrophysical Science Center, Hiroshima University, Higashi-Hiroshima, Hiroshima, Japan
[5] Optical and Infrared Astronomy Division, National Astronomical Observatory, Mitaka, Tokyo, Japan
[6] Subaru Telescope, National Astronomical Observatory of Japan, Hilo, HI
[7] Istituto Naz. di Astrofisica-Oss. Astron., Via Tiepolo, 11, 34131 Trieste, Italy
[8] Max-Planck Institut für Astrophysik, Karl-Schwarzschild-Strasse 2 D-85748 Garching bei München, Germany
[9] Istituto Naz. di Astrofisica-Oss. Astron., vicolo dell'Osservatorio, 5, 35122 Padova, Italy
[10] Department of Physics, Konan University, Okamoto, Kobe, Japan

maximum (Maeda et al. 2007).

In order to explain the two peaks of the light curve by radioactivity, the distribution of ^{56}Ni must have two components. This fact led Tominaga et al. (2005) and Folatelli et al. (2006) to propose a jet-like explosion for SN 2005bf. However, the low luminosity at nebular phases may suggest another heating source for the second peak, such as central remnant's activity (Maeda et al. 2007).

Maund et al. (2007a) (hereafter M07) presented a spectropolarimetric observation of SN 2005bf taken with the Very Large Telescope (VLT) at 6 days before the second visual maximum, i.e., at $t = -6$ days, where t indicates the epoch relative to the second visual maximum, JD 2453498.8 (Folatelli et al. 2006). Based on detected large polarization levels and changes in the polarization position angle at the lines of He I, Ca II and Fe II, they suggested a tilted-jet model, i.e., a scenario in which the asphericity is due to the ejection of blob(s) (or jets) in a tilted direction with respect to the symmetry axis of the SN.

One difficulty in polarimetric observations is accounting for the degree of interstellar polarization (ISP) caused by interstellar extinction (Davis & Greenstein 1951). Although a correct estimate of ISP is essential to determine the intrinsic polarization of the SN, such an estimate is especially difficult to determine with an observation at a single epoch.

We present spectropolarimetric data of SN 2005bf taken with the 8.2 m Subaru telescope at 14 days after the observation by M07. The two-epoch data enable us to estimate ISP more carefully. In §2, we present the observations and data reduction. The data taken at the two epochs are compared, and updated estimates of ISP are shown in §3. In §4, our interpretation of spectropolarimetric data is discussed. Finally, we give the conclusions in §5.

2. OBSERVATIONS AND DATA REDUCTION

Spectropolarimetry of SN 2005bf was performed with the 8.2 m Subaru telescope equipped with the Faint Object Camera and Spectrograph (FOCAS, Kashikawa et al. 2002) on 2005 May 15 UT (JD 2453506.76). This epoch corresponds to $t = +8$ days (14 days after the observation by M07).

We used a slit of $0.8''$ width and two 300 lines mm^{-1} grisms. Blue ($\lambda < 6900$ Å) and red ($\lambda > 6900$ Å) spectra were taken separately. No filter was used for the blue spectrum, while the O58 filter was used for the red spectrum to eliminate the second order light. The wavelength resolution is $\lambda/\Delta\lambda \sim 650$.

The linear polarimetric module of FOCAS consists of a rotating superachromatic half-wave plate and a crystal quartz Wollaston prism. Both the ordinary and extraordinary rays are recorded on the CCD simultaneously. From four integrations at the 0°, 45.°, 22.5° and 67.5° positions of the half-wave plate, Stokes Q and U were derived as in Tinbergen (1996). The total exposure time of four integrations was 2400 sec for each part of the spectrum.

The position angle was calibrated by the observation of the strongly polarized star HD 155197 (Turnshek et al. 1990). The wavelength dependence of the optical axis of the half-wave plate was also corrected using this observation. Since sky conditions were better during the observation of the blue spectrum, the polarization data are binned into 30 Å and 50 Å for the blue and red spectra, respectively. This yields an average signal-to-noise ratio S/N $\sim$ 330. For the degree of polarization P, the polarization bias was corrected using the results of Patat & Romaniello (2006).

The flux spectrum was calibrated using the observation of the spectrophotometric standard star Feige34 (Oke 1990) and further calibrated using previously reported photometry of the SN (Tominaga et al. 2005). Telluric absorption lines are removed using the spectrum of the standard star.

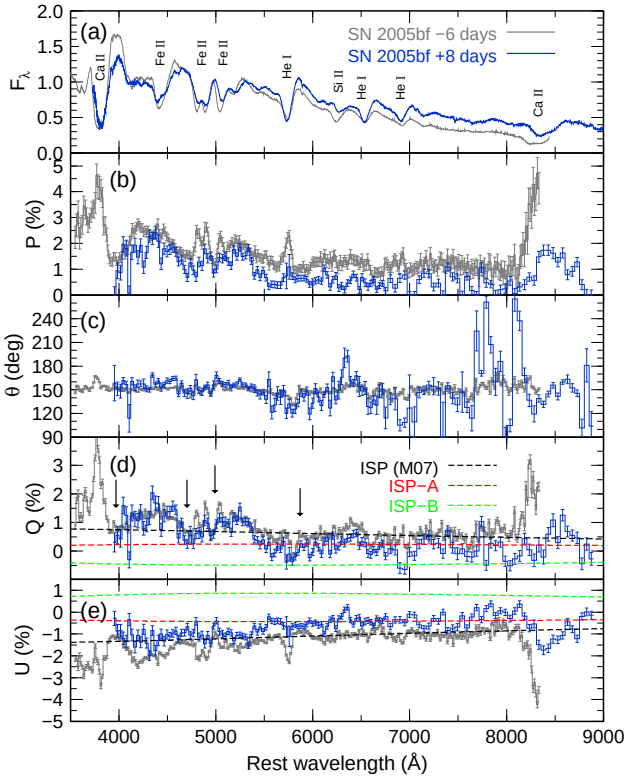

FIG. 1.— (a) Spectrum of SN 2005bf (blue, 10^{-15}erg s^{-1} cm^{-2} Å^{-1}) at $t = +8$ days from the second visual maximum (JD 2453498.8, Folatelli et al. 2006) compared with the scaled spectrum at $t = -6$ days (gray, M07); (b) bias-corrected polarization P; (c) polarization angle θ; (d, e) the Stokes parameters Q and U. P, Q, U, and θ have *not* been corrected for Interstellar polarization (ISP). The black dashed line shows the ISP assumed by M07 while the red and green dashed line shows our updated estimates. The arrows in panel (d) show the position of the emission peak of strong lines, where complete depolarization is assumed. The data at $t = +8$ days taken with the Subaru telescope are binned to 30 Å and 50 Å for the bluer ($\lambda < 6900$Å) and redder ($\lambda > 6900$Å) parts of the spectrum. The data at $t = -6$ days taken with VLT (M07) are binned to 15 Å.

3. RESULTS

3.1. *Spectropolarimetric Properties at the Two Epochs*

Figure 1 shows comparison of flux spectrum and polarization spectrum at $t = +8$ days (blue) with those at $t = -6$ days (gray). Line identifications are given in the panel for the total light spectrum (a). It is interesting to note that He line velocities increase with time (Tominaga et al. 2005). This is in contrast to the usual behavior, i.e., the photosphere recedes and line veloci-

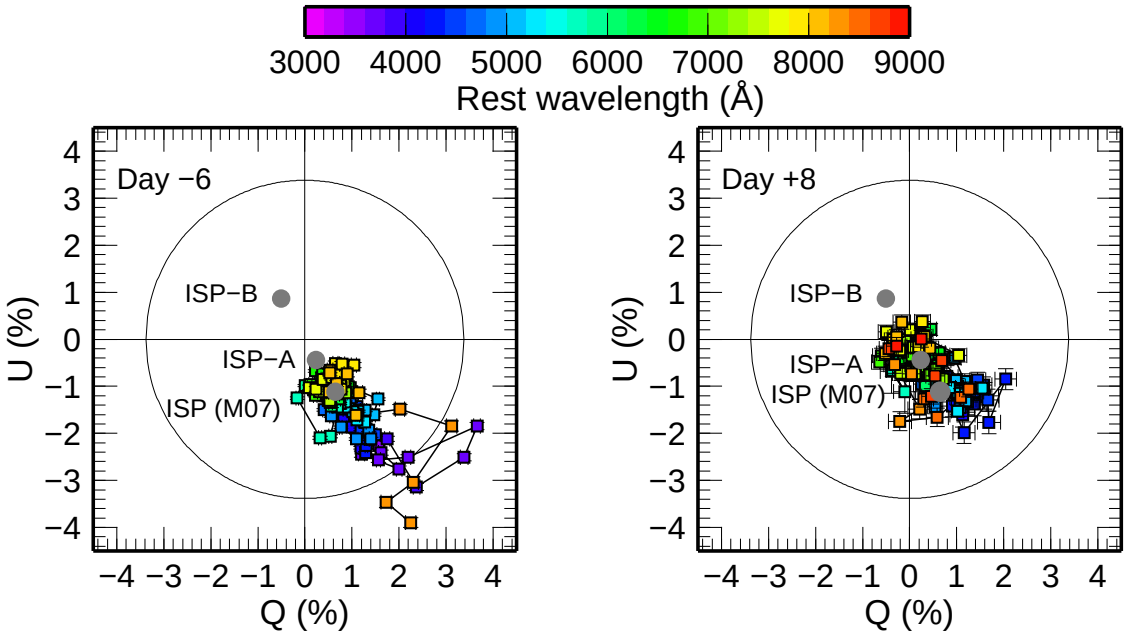

FIG. 2.— *Q-U* diagram of the polarization data before correction of ISP. *Left*: The VLT data taken at $t = -6$ days by M07. The data are binned to 30 Å. *Right*: The Subaru data taken at $t = +8$ days. The data are binned to 30 Å and 50 Å for the blue and red spectra, respectively. Different colors show the wavelength according to the color scale bar. The ISPs at 5500 Å estimated by M07 and by this work are marked with gray circles. The large circle shows the upper limit for the ISP (3.4%).

ties decrease with time in expanding ejecta. This peculiar behavior of SN 2005bf may suggest increasing non-thermal excitation of the He lines (Harkness et al. 1987; Lucy 1991).

The Stokes Q parameter at $t = +8$ days is smaller than that at $t = -6$ days in the continuum (d). The difference in the Ca II triplet region is larger than in the continuum. The difference in the Stokes U parameter between the two epochs is more prominent than Q over the whole wavelength range (e). The U parameter at $t = +8$ days is larger than that at $t = -6$ days (about half in absolute value).

The difference in the Stokes Q and U between the two epochs is more easily seen in the Q-U plane (Fig. 2). In the Q-U plane, the data at $t = +8$ days are closer to zero point. The position angle is similar at the two epochs, $\theta \sim 150°$ [$\theta \equiv 0.5\mathrm{atan}(U/Q)$, see also panel ($c$) of Fig. 1].

As a result, the degree of polarization [$P \equiv (Q^2 + U^2)^{1/2}$] is smaller at $t = +8$ days over the whole wavelength range (panel (b) of Fig. 1). In the line-free region, the difference in the polarization is $\sim 0.5\%$. The polarization at the strong lines, e.g., He I λ5876, Ca II IR triplet and Fe II lines at 4300-5100 Å is also smaller at $t = +8$ days. In particular, the polarization in the Ca II triplet region decreases by a factor of > 2 in absolute value.

Multi-epoch spectropolarimetry of Type Ib/c SNe has not been performed for many objects (Wang & Wheeler 2008). One of the well-observed example is Type Ic SN 2002ap. For SN 2002ap, the continuum polarization level increases with time before the maximum brightness (Wang et al. 2003a). After maximum, the polarization decreases or it is almost unchanged (Kawabata et al. 2002; Leonard et al. 2002; Wang et al. 2003a). For SN 2005bf, polarization decreases in the interval from $t = -6$ to $+8$ days. However, since we don't know the polarization around the maximum, the time evolution could possibly be similar to that of SN 2002ap [11].

3.2. *Updated Estimates of Interstellar Polarization*

To discuss intrinsic properties of SN polarization, polarization caused by interstellar extinction (ISP) must be corrected. First, we give an upper limit of ISP by the total amount of reddening (Serkowski et al. 1975). In the line of sight to SN 2005bf, Galactic extinction is $E(B-V) = 0.01$ mag (Schlegel et al. 1998). M07 estimated the extinction by the host galaxy to be $E(B-V) < 0.37$ mag by using the equivalent width of the Na I D line and the relation given by Turatto et al. (2003). Thus, the relation of $P/E(B-V) < 9\%$ (Serkowski et al. 1975) gives the maximum degree of ISP $P < 3.4$ %. This maximum value is shown by the large circle in Figure 2.

The wavelength dependence of ISP is represented by

$$p(\lambda) \;=\; p_{\max} \exp\left[-K \,\ln^2\left(\lambda_{\max}/\lambda\right)\right], \qquad (1)$$

which is valid for the Milky Way-like dust (Serkowski et al. 1975). Here $\lambda_{\max}$ is the wavelength at the peak of ISP, $p_{\max}$ is the degree of ISP at $\lambda_{\max}$, and K is given as $K = 0.01 + 1.66\ \lambda_{\max}$ (μm) (Whittet et al. 1992). M07 estimated ISP (the black dashed lines in Fig. 1) by assuming complete depolarization at the emission peak of He I, Ca II and Fe II lines (marked by arrows in panel (d) of Fig. 1). This is often assumed when ISP must be estimated from a

[11] A decreasing trend in polarization is reported for Type Ic SN 2006aj associated with X-ray flash 060218 (Gorosabel et al. 2006), although the observation consists only in imaging polarimetry [see Maund et al. 2007b for a single-epoch spectropolarimetry of SN 2006aj].

single epoch spectropolarimetry. As a result, ISP was estimated as $p_{\rm max} = 1.6 \pm 0.2$ %, $\lambda_{\rm max} = 3000$ Å, and $\theta_{\rm ISP} = 149.7° \pm 4.0°$.

However, our data show that the assumption of the complete depolarization at $t = -6$ days is not necessarily true. The polarization levels at the emission peak of the Fe II lines and He I λ5876 are different between $t = -6$ and +8 days. This fact indicates that the contribution of ISP should be smaller, as already cautioned by M07.

ISP can be estimated more carefully from multi-epoch data. The position angle is similar at the two epochs. This fact suggests that the position angle of ISP is $\theta \sim 150°$ (similar to the position angle of the observed data) or 60° (the opposite side in the Q-U plane) if the SN does not have a complex change of position angle. If the position angle of ISP were far from the above two values, the intrinsic SN polarization would have a complex wavelength dependence and a time dependence.

If we take a position angle of ISP $\theta_{\rm ISP} = 149.7°$ as in M07, a new upper limit of ISP can be obtained by fitting the polarization at the emission peak of strong lines at $t = +8$ days, e.g., He I λ5876, Ca II H&K and IR triplet and Fe II lines. Under the conventional assumption of $\lambda_{\rm max} = 5500$ Å, good simultaneous fits are obtained with $p_{\rm max} = 0.5 \pm 0.1$ %. This is shown with the red dashed lines in Figure 1 and in the gray circle in Figure 2. We call this upper limit ISP-A.

It should be noted, however, that the position angle of ISP-A is orthogonal to the spiral arm of the host galaxy (see Fig. 1 of M07). This is in contradiction to the expectation that ISP is aligned with the spiral arm due to the alignment of dusts by the magnetic field (Scarrott et al. 1987, 1993). Thus, it is also quite likely that ISP has a position angle $\theta_{\rm ISP} \sim 60°$, being aligned with the spiral arm. In addition, this does not cause any complex change in the position angle of SN (see above). In this case, the degree of ISP is only weakly constrained by the total extinction, i.e., $P < 3.4\%$. We take $p_{\rm max} = 1\%$ as an example. This ISP, hereafter denoted as ISP-B, is shown in the green dashed lines in Figure 1 and in the gray circle in Figure 2. Since the correct value of $p_{\rm max}$ is unclear, it is cautioned that the exact value of the intrinsic polarization is also arbitrary.

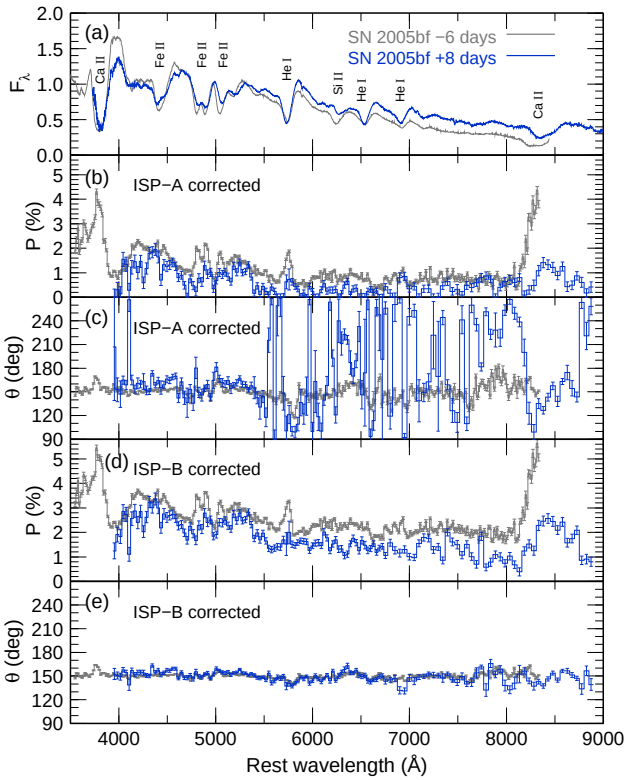

FIG. 3.— (a) Spectra of SN 2005bf at $t = +8$ days (blue, in 10^{-15}erg s^{-1} cm^{-2} Å^{-1}) and at $t = -6$ days (gray, in scaled flux). (b, c) polarization and position angle corrected with ISP-A. (d, e) polarization and position angle corrected with ISP-B. ISP-A is an upper limit of ISP when the position angle is $\theta_{\rm ISP} = 149.7°$ ($p_{\rm max} = 0.5\%$ and $\lambda_{\rm max} = 5500$ Å). ISP-B is an example case where the position angle of ISP is aligned with the spiral arm of the host galaxy: $p_{\rm max} = 1.0\%$, $\lambda_{\rm max} = 5500$ Å, and $\theta_{\rm ISP} = 60°$.

4. ASYMMETRY OF SN 2005bf

Figure 3 shows polarization and position angle corrected with ISP-A (b, c) and ISP-B (d, e). We discuss asymmetric geometry of SN 2005bf inferred from the two-epoch spectropolarimetric data and other observational facts.

4.1. *Continuum Polarization*

Intrinsic continuum polarization (defined in the line-free region at 7000-8000 Å) at $t = -6$ days was estimated as ~ 0.45 % under the assumption of ISP by M07. However, with our updated ISP estimates, it is at least 0.8% (Fig. 3). Using the results of Höflich (1991), with the opacity at the photosphere $\tau = 1$ and oblate geometry, this suggests that the axis ratio of the photosphere projected on the sky deviates from unity by ~ 20 %.

If the position angle of ISP is aligned with the spiral arm of the host galaxy, intrinsic continuum polarization is $\gtrsim 1.2\%$. This suggests even larger asymmetry of the photosphere, being $\gtrsim 25\%$. Since $p_{\rm max}$ is not strongly constrained in this case, the intrinsic polarization is uncertain. For example, under the assumption of ISP-B ($p_{\rm max} = 1\%$), the axis ratio can be deviated from unity by as large as 50 %.

After the correction of ISP, the difference in the polarization between the two epochs is larger in the redder part than in the bluer. This could indicate that the ISP peaks at bluer than 5500 Å as suggested by M07.

The intrinsic polarization level at $t = +8$ days largely depends on the choice of ISP. If the position angle of ISP is $\theta_{\rm ISP} \sim 60°$, the continuum polarization at $t = +8$ days is $> 0.5\%$. The variation of the position angle along the wavelength is very small since $\theta_{\rm ISP} = 60°$ is aligned with the observed data in the Q-U plane. In addition, the agreement in the position angle at two epochs is extremely good when ISP-B is corrected (panel (e) in Fig. 3). This is because ISP-B is out of scatter around the zero point in the Q-U plane at $t = +8$ days. These facts may support the possibility that the position angle of ISP is aligned with the spiral arm of the host galaxy. Although $p_{\rm max}$ is quite uncertain in the case of $\theta_{\rm ISP} = 60°$, $p_{\rm max} > 0.5\%$ may be preferable to avoid a complex wavelength-dependence of the position angle of the SN at $t = +8$ days.

Since the interval of the two epochs is not close, the exact evolution of the continuum polarization is not clear. It is true, however, that the polarization is smaller at

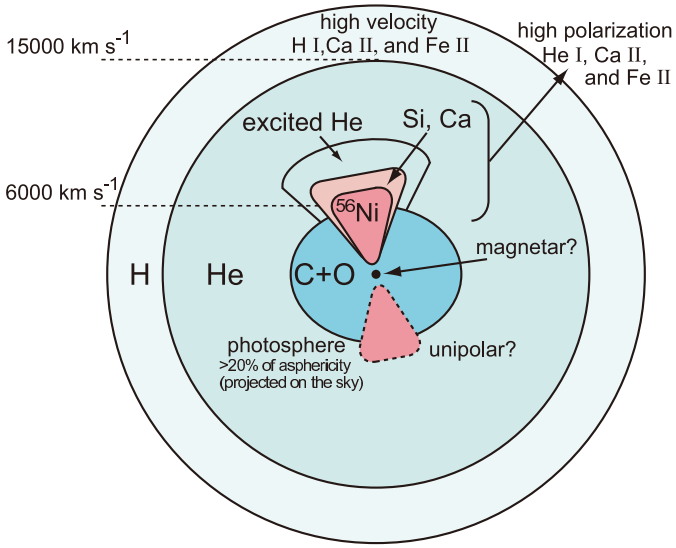

FIG. 4.— Schematic illustrations of an aspherical explosion model for SN 2005bf. Our line of sight is near the polar direction. The progenitor star is a WN star with a thin H layer. High velocity Ca II and Fe II lines are formed in the H layer. The He layer is located at 6,000 - 15,000 km s^{-1}. The blob of ^{56}Ni penetrates the C+O core, but not the He layer. Synthesized, asphericallydistributed ^{56}Ni and Ca may be responsible for the high polarization level of the Ca II and Fe II lines. The line forming region of He I is also aspherical because of the selective excitation around the ^{56}Ni blob. The photosphere is deformed by the aspherical ejection of the blob or jets. The axis ratio of the photosphere projected on the sky deviates from unity by least 20 %. The direction where the blob is ejected is tilted with respect to the symmetry axis of the photosphere (M07). The explosion could possibly be unipolar as suggested by the shift of the nebular emission lines (Maeda et al. 2007).

the later epoch. This can be understood by (1) decreasing optical depth of electron scattering or (2) decreasing asphericity of the photosphere. In optically thin case, the effect of (1) is important, as observed after plateau phase of Type II SNe (Leonard et al. 2006). However, the epoch of our observation seems to be earlier than the epoch when the transition to the nebular phase happens. Thus, the actual change of the photospheric shape (2) could also be likely.

4.2. *Line Polarization*

At both epochs, a large polarization is observed at the He I λ5876, Ca II IR triplet and Fe II lines. Little polarization is seen at the He I λ6678 and λ7065, but this may be due to the weakness of these lines. The line polarizations at strong lines at $t = +8$ days are smaller than at $t = -6$ days. This can be caused partly by the smaller polarization of the underlying photospheric radiation at the later epoch.

The difference of the polarization between the two epochs is the largest at the Ca II IR triplet region among three strong lines. The large change may suggest that asphericity of the Ca II distribution depends on the velocity (radius), i.e., larger asphericity in the outer layers. Since the change in the velocities of the He I and Fe II lines is smaller than that in the Ca II line, the radial dependence of asphericity cannot be discussed for the He and Fe.

M07 discussed the change in the position angle at the He I, Ca II and Fe II lines. This appears as a loop in the Q-U plane and indicates that the photosphere and the line forming region do not share a common symmetry axis. At $t = +8$ days, the change in the position angle at these lines is also seen at the Ca II line, and marginally at the He I and Fe II lines, although the loop in the Q-U plane is not as prominent as that at $t = -6$ days. The similar polarimetric behaviors of these lines, i.e., the similar position angle especially under ISP-B and the smaller polarization level at the later epoch, suggest that the distributions of these ions are correlated.

At both epochs, no strong polarization is observed at the Si II λ6355 and the O I λ7774. Since these lines are very weak, no detection of polarization does not necessarily indicate sphericity of the distribution of Si II and O I. Although M07 discussed polarization of H lines, the H lines are not clearly identified at $t = +8$ days (see Folatelli et al. 2006).

4.3. *Aspherical Explosion Model*

We discuss explosion geometry of SN 2005bf. To explain spectropolarimetric behaviors as well as the behaviors of the light curve and spectra both at photospheric ($\lesssim 70$ days after the explosion) and nebular (~ 1 year after the explosion) phases, we suggest an aspherical model as illustrated in Figure 4.

The progenitor star of SN 2005bf is suggested to be a WN star by the identification of the high velocity Hα line (Anupama et al. 2005; Tominaga et al. 2005; Folatelli et al. 2006). The velocity at the bottom of the H layer is $\sim 15,000$ km s^{-1}.

The He layer is located below the H layer. The velocity at the bottom of the He layer is around 6,000 km s^{-1}, constrained by the minimum velocities of the He lines (Tominaga et al. 2005). Since the velocities of the He lines increase with time, it is suggested that the excitation of He I grows with time. Thus, ^{56}Ni is not completely mixed with the He layer. The distribution of ^{56}Ni is clumpy, which is suggested by the high polarization level of the Fe lines. Around the ^{56}Ni blob, non-thermal electrons are created by Compton scattering of γ-rays emitted in the decay of ^{56}Ni and ^{56}Co. Thus, the He lines are formed around the ^{56}Ni blob.

Heavy elements such as Si and Ca must also be synthesized around ^{56}Ni. The polarization of the Ca II line that depends on the velocity (radius, §4.2) could be explained by the flared distribution of synthesized, heavy elements as illustrated in Fig. 4, which is often seen in simulations of jet-like explosion (e.g., Tominaga 2009). Since the absorption of Si is very weak, no detection of polarization at the Si line is not inconsistent with this geometry. The geometry discussed above can explain the similar polarization properties of the He I, Ca II, and Fe II lines.

The C+O core is located below the He layer at 6,000 km s^{-1}. The photosphere at $t = -6$ and $+8$ days is located in the C+O core (Tominaga et al. 2005). The photosphere is deformed so that the projected photosphere has $> 20\%$ asymmetry. This degree of asphericity can be formed by the ejection of the blob (or jets) toward the polar region (e.g., Khokhlov et al. 1999; Maeda et al. 2002). However, the photosphere and the distribution of ^{56}Ni do not share a common symmetry axis as suggested by the changes in the position angle across the lines. This could be due to the fact that the direction where the blob

is ejected is tilted with respect to the symmetry axis of the photosphere (as in a tilted-jet model suggested by M07). Such distributions could possibly be realized by, for example, a magnetorotational explosion, where the rotational axis is inclined with respect to the magnetic field (Mikami et al. 2008).

The ^{56}Ni blob toward us is responsible for the first peak of the light curve (Maeda et al. 2007). It may also explain the velocity shifts of the emission lines seen in the nebular spectra. In this case, the explosion may be unipolar. In addition, the second peak of the light curve is powered by another heating source. Maeda et al. (2007) proposed magnetar as a central remnant of SN 2005bf and reproduced the observed light curve until late phases.

Folatelli et al. (2006) and Parrent et al. (2007) suggested that the high velocity Ca II and Fe II lines that were present at early epochs ($t \lesssim -20$ days) support the jet-like explosion. However, since the velocities of these lines coincide to that of Hα ($v \sim 15,000$ km s^{-1}), the high velocity Ca II and Fe II lines are formed in the H layer. If the jet or blob-like structure does not penetrate the He layer as illustrated in Figure 4, these lines are unlikely to be associated with the blob. Alternatively, these high velocity lines can result from the solar abundance in the H layer because of a high electron density in the H layer, enhancing the recombination of Ca III and Fe III (Mazzali et al. 2005; Tanaka et al. 2008b).

5. CONCLUSIONS

We have presented an optical spectropolarimetric observation of the unique Type Ib SN 2005bf taken with the Subaru telescope at $t = +8$ days. Comparison with the data taken with VLT at $t = -6$ days enables us to closely study the intrinsic properties of the SN.

Polarization at $t = +8$ days is smaller than that at $t = -6$ days, with an almost constant position angle at a wide wavelength range. We find that an assumption of complete depolarization at the emission peak of strong lines is not necessarily correct. This requires reanalysis of the ISP contribution in the observed data. We put a smaller upper limit for ISP. Thus, the intrinsic polarization of the SN is larger, i.e., the ejecta of SN 2005bf would be more asymmetric. The axis ratio of the photosphere projected on the sky deviates from unity by at least 20%.

It is likely that the position angle of ISP is aligned with the spiral arm of the host galaxy. If this is the case, the continuum polarization at $t = -6$ days is at least $\sim 1.2\%$. Then the asymmetry of the projected photosphere is even larger, being $\gtrsim 25\%$.

The degrees of the line polarization at the He I, Ca II and Fe II lines similarly decrease from $t = -6$ to $+8$ days. The change in the position angle across the line, making a loop in the Q-U plane, is seen in the Ca II line and also marginally in the He I and Fe II lines at $t = +8$ days. The similar behavior of these lines suggests that the distribution of these ions are correlated.

We propose an aspherical, possibly unipolar explosion model of a WN star as shown in Figure 4. In this model, the ^{56}Ni-rich blob penetrates C+O core and stops within the He layer. The direction in which the ^{56}Ni-rich blob is ejected is tilted with respect to the symmetry axis of the aspherical photosphere (M07). The blob is responsible for the first peak of the light curve. If the explosion is unipolar, the shifted nebular emission lines are also explained by the blob (Maeda et al. 2007). The non-thermal electrons originating from the ^{56}Ni-rich blob selectively excite He around the blob, and this configuration can explain the similar polarization properties of the He I, Ca II and Fe II lines.

We are grateful to the staff of the Subaru Telescope for their kind support. We thank Justyn Maund and the co-authors of Maund et al. (2007a) paper for kindly providing their polarization data taken with VLT (ESO VLT program 75.D-0213). We are also grateful to the staff of VLT. M.T. and N.T. are supported by the JSPS (Japan Society for the Promotion of Science) Research Fellowship for Young Scientists. This research has been supported in part by World Premier International Research Center Initiative, MEXT, Japan, and by the Grant-in-Aid for Scientific Research of the JSPS (18104003, 18540231, 20540226) and MEXT (19047004, 20040004).

REFERENCES

Anupama, G. C., Sahu, D. K., Deng, J., Nomoto, K., Tominaga, N., Tanaka, M., Mazzali, P. A., & Prabhu, T. P. 2005, 631, 125
Blondin, J.M., Mezzacappa, A., & DeMarino, C., 2003, ApJ, 584, 971
Burrows, A., Hayes, J., Fryxell, B. A. 1995, ApJ, 450, 830
Cropper, M., Bailey, J., McCowage, J., Cannon, R. D., & Couch, Warrick J. 1988, MNRAS, 231, 695
Davis, L. Jr., Greenstein, J. L. 1951, ApJ, 114, 206
Folatelli, G., et al. 2006, ApJ, 641, 1039
Gorosabel, J., et al. 2006, A&A, 459, L33
Harkness, R. P., et al. 1987, ApJ, 317, 355
Hoffman, J. L., Leonard, D. C., Chornock, R., Filippenko, A. V., Barth, A. J., Matheson, T. 2008, ApJ, 688, 1186
Höflich, P. 1991, A&A, 246, 481
Hwang, U., et al. 2004, ApJ, 615, L117
Iwakami, W., Kotake, K., Ohnishi, N., Yamada, S., & Sawada, K 2008, ApJ, 678, 1207
Janka, H.-Th., Müller, E. 1996, A&A, 306, 167
Kashikawa, N., et al. 2002, PASJ, 54, 819
Kawabata, K.S., et al. 2002, ApJ, 580, L39
Kawabata, K.S., et al. 2003, ApJ, 593, L19
Khokhlov, A. M., Höflich, P. A., Oran, E. S., Wheeler, J. C., Wang, L., & Chtchelkanova, A. Yu. 1999, ApJ, 524, L107
Leonard, D.C., Filippenko, A. V., Ardila, D. R., & Brotherton, M. S. 2001, ApJ, 553, 861
Leonard, D.C., Filippenko, A.V., Chornock, R., & Foley, R. 2002, PASP, 114, 1333
Leonard, D.C., et al. 2006, Nature, 440, 505
Lucy, L. B. 1991, ApJ, 383, 308
Maeda, K., et al. 2002, ApJ, 565, 405
Maeda, K., et al. 2007, ApJ, 666, 1069
Maund, J. R., Wheeler, J. C., Patat, F., Baade, D., Wang, L., & Höflich, P. 2007a, MNRAS, 381, 201 (M07)
Maund, J. R., Wheeler, J. C., Patat, F., Baade, D., Wang, L., & Höflich, P. 2007b, A&A, 475, L1
Maund, J. R., Wheeler, J. C., Patat, F., Wang, L., Baade, D., Höflich, P. A. 2007c, ApJ, 671, 1944
Mazzali, P.A. Benetti, S., Stehle, M., Branch, D., Deng, J., Maeda, K., Nomoto, K., & Hamuy, M. 2005, MNRAS, 357, 200
McCall, M. L. 1984, MNRAS, 210, 829
Mikami, H., Sato, Y., Matsumoto, T., & Hanawa, T. 2008, ApJ, 683, 357
Modjaz, M., Kirshner, R.P., & Challis, P. 2005, IAU Circ., 8522, 2
Müller, E., & Hillebrandt, S. 1981, A&A, 103, 358
Oke, J.B. 1990, AJ, 99, 1621
Parrent, J., et al 2007, PASP, 119, 135
Patat, F. & Romaniello, M., 2006, PASP, 118, 146
Scarrott, S. M., Ward-Thompson, D., & Warren-Smith, R. F. 1987, MNRAS, 224, 299

Scarrott, S. M., Draper, P. W., Stockdale, D. P., & Wolstencroft, R. D., 1993, MNRAS, 264, L7
Serkowski, K., Mathewson, D.L., & Ford, V.L. 1975, ApJ, 196, 261
Schlegel, D. J., Finkbeiner, D. P., & Davis, M. 1998, ApJ, 500, 525
Shapiro, P.R., & Sutherland, P.G. 1982, ApJ, 263, 902
Takiwaki, T., Kotake, K., Nagataki, S., & Sato, K. 2004, ApJ, 616, 1086
Tanaka, M., Kawabata, K. S., Maeda, K., Hattori, T., & Nomoto, K. 2008a, ApJ, 689, 1191
Tanaka, M., et al. 2008b, ApJ, 677, 448
Tinbergen, J. 1996, Astronomical Polarimetry (New York: Cambridge Univ. Press)
Tominaga, N., et al. 2005, ApJ, 633, L97
Tominaga, N., 2009, ApJ, 690, 526
Trammell, S.R., Hines, D.C., & Wheeler, J.C. 1993, ApJ, 414, L21
Turatto M., Benetti S., Cappellaro E., 2003, in From Twilight to Highlight: The Physics of Supernovae, ed. by Hillebrandt W., Leibundgut B., Springer, Berlin, 200
Turnshek, D. A., Bohlin, R. C., Williamson, R. L., II, Lupie, O. L., Koornneef, J., & Morgan, D. H. 1990, AJ, 99, 1243
Wang, L., et al. 2001, ApJ, 550, 1030
Wang, L., et al. 2002, ApJ, 579, 671
Wang, L., Baade, D., Höflich, P., & Whheler, J.C 2003, ApJ, 592, 457
Wang, L., & Baade, D. 2005, IAU Circ., 8521, 2
Wang, L., & Wheeler, J. C. 2008, ARA&A, 46, 433
Whittet, D. C. B., Martin, P. G., Hough, J. H., Rouse, M. F., Bailey, J. A., & Axon, D. J. 1992, ApJ, 386, 562
Yamada, S., & Sato, K. 1994, ApJ, 434, 268